doi:10.1038/nature12158

1. Numerical retrieval of effective parameters of metamaterial

We perform FDTD simulations of an unmasked, free-standing slab of as-designed metamaterial (thickness d = 450 nm), illuminated by a transverse-magnetic-polarized (TMP) plane-wave (λ_0 = 363.8 nm), at various angles of incidence θ_i. The refractive indices for Ag ($n = 0.0785 + 1.59\,i$) and TiO_2 ($n = 2.8 + 0.05\,i$) used in the simulations are obtained from ref. 1 and spectroscopic ellipsometry measurements, respectively. Effective parameter retrieval[2] then yields, as a function of θ_i, the complex effective electric permittivity, $\underline{\varepsilon}_{eff}$, the complex effective magnetic permeability, $\underline{\mu}_{eff}$, and the complex effective mode index, $\underline{n}_{m,eff}$ of the metamaterial (Fig. 1). The real parts of $\underline{\varepsilon}_{eff}$ (Fig. 1a) and $\underline{\mu}_{eff}$ (Fig. 1b) are simultaneously negative over the explored angular range $0^\circ \le \theta_i \le 70^\circ$, yielding a classical double-negative left-handed medium. As shown in Fig. 1c, the effective refractive index of the metamaterial, $n_{eff} = \mathrm{Re}(\underline{n}_{m,eff})$, is negative and relatively constant over the range $0^\circ \le \theta_i \le 70^\circ$ (monotonically decreasing from –0.96 at $\theta_i = 0^\circ$ to -1.07 at $\theta_i = 70^\circ$), confirming an all-angle left-handed response characterized by a refractive index close to the targeted value of -1. The simulated figure of merit (FOM) of the metamaterial, defined as $\left|\mathrm{Re}[\underline{n}_{m,eff}]/\mathrm{Im}[\underline{n}_{m,eff}]\right|$, takes on a range of values (from 4 at $\theta_i = 0^\circ$ to 5.7 at $\theta_i = 70^\circ$) which are all relatively high compared to the typical FOM of conventional resonator-based metamaterials not incorporating gain media.

The imaginary parts of $\underline{\varepsilon}_{eff}$ (Fig. 1a) and $\underline{\mu}_{eff}$ (Fig. 1b) are respectively positive and negative. Like other metamaterials reported to have values of $\varepsilon'' \equiv \mathrm{Im}(\varepsilon)$ and $\mu'' \equiv \mathrm{Im}(\mu)$ of opposite signs[3,4], the present metamaterial seems to contradict the thermodynamic requirement of positive energy dissipation, commonly interpreted as $\varepsilon'' > 0$ and $\mu'' > 0$ (ref. 5). Recent work has suggested, however, that the condition of positive energy dissipation does not necessarily require that ε'' and μ'' be simultaneously positive[6] and that it is nonetheless possible to satisfy thermodynamic requirements while still having one of ε'' or μ'' be negative.

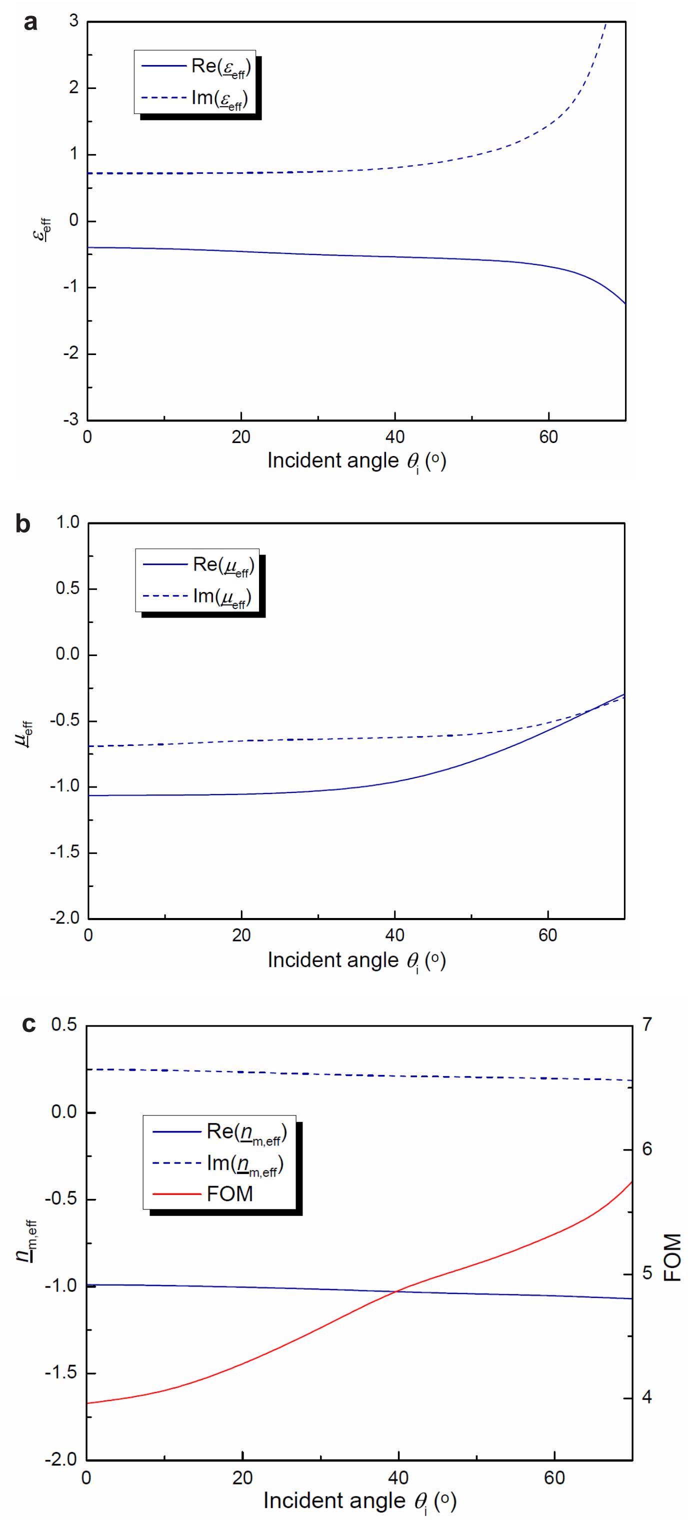

Figure 1 | Retreived effective medium parameters of metamaterial. a, Complex effective permittivity, ε_{eff} . **b,** complex effective permeability, μ_{eff} . **c,** complex effective mode index, $n_{m,eff}$ (left-axis), and corresponding figure of merit, FOM (right-axis), plotted as a function of incident angle θ_i . TMP illumination. Wavelength: $\lambda_0 = 363.8$ nm.

2. Simulated resolution limit of implemented flat-lens

The theoretical resolution limit of the experimentally-implemented flat lens is investigated via FDTD simulations of a free-standing slab of as-designed metamaterial (thickness d = 450 nm) illuminated at normal incidence by a plane-wave source (λ_0 = 363.8 nm) of subwavelength width, w_s, placed directly on the input surface of the slab. The refractive indices assumed for the constituent Ag and TiO_2 layers are identical to those quoted in the previous section. The image of the truncated plane wave projected by the flat lens is characterized for values of w_s spanning the range 30 to 300 nm. The simulated total energy density reveals an image beam waist located at a distance z_f = 360 nm from the lens exit surface. The image width, $w_{f,FDTD}$, defined as the FWHM of the energy-density waist at z_f, is plotted in Fig. 2 as a function of w_s . As the source-width w_s decreases towards zero, the image width $w_{f,FDTD}$ decreases towards a limit of $\approx$190 nm. This value is larger than, but relatively close to the minimum image width of 161 nm (FWHM) theoretically predicted to result when a line source of infinitesimal width is imaged at $\lambda_0 = 363.8$ nm by a free-space diffraction-limited system having a maximal value of numerical aperture (N.A. = 1).

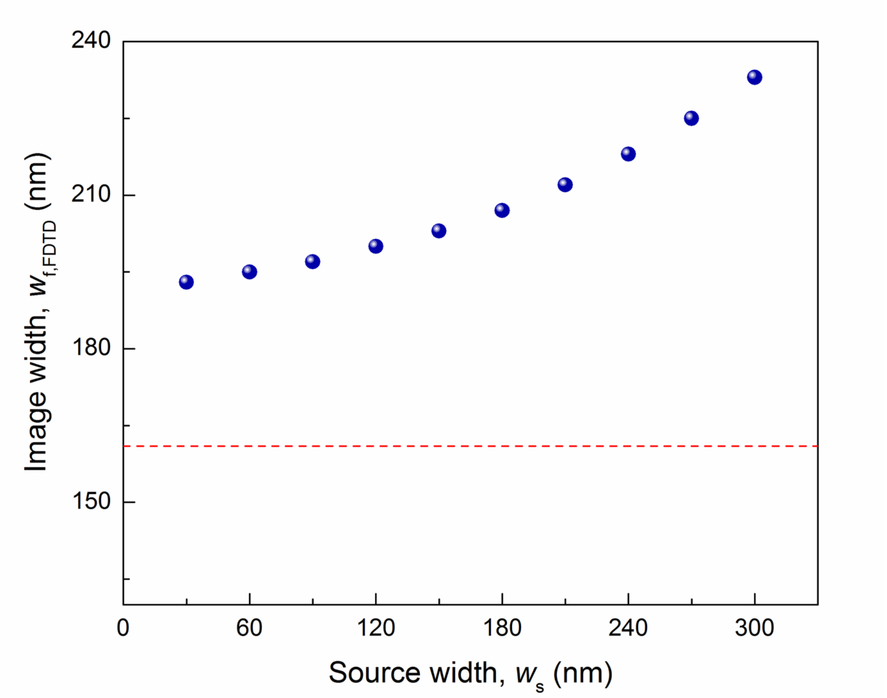

Figure 2 | Simulated resolution of the flat lens. The blue dots show the FDTD-simulated image width, $w_{f,FDTD}$, as a function of source width, w_s. The red dashed line indicates the predicted image width for a line source imaged by a diffraction-limited system with N.A. = 1. Lens thickness: d = 450 nm. Operating wavelength: λ_0 = 363.8 nm.

3. Active flat lensing: TiO_2 optical properties and experimental setup

To infer the bandgap of the TiO_2 semiconducting material incorporated in the experimental flat lens, a UV-Visible spectrometer was used to measure the optical absorbance spectrum of a 50nm-thick TiO_2 reference film sputter-deposited onto a fused-quartz slide (Fig. 3a). The onset of a distinct absorption-edge is observed at a wavelength of $\approx$ 350 nm (as a function of decreasing wavelength), implying an experimental TiO_2 bandgap of value $E_{BG} \approx 3.54$ eV.

Fig. 3b shows the schematic diagram of the experimental setup used to demonstrate active flat lensing. To generate free carriers to suppress the optical transmission of the metamaterial slab at its designed working wavelength of 363.8 nm, an above-bandgap pump beam of wavelength $\lambda_{pump} = 290$ nm is chosen. In a control experiment intended to verify the lack of transmission suppression in the absence of optically-generated free carriers, a sub-bandgap pump beam of wavelength $\lambda_{pump} = 760$ nm is used instead.

Supplementary References

1. Johnson, P. B. & Christy, R. W., Optical constants of the noble metals. *Phys. Rev. B* **6**, 4370-4379 (1972).

2. Menzel, C. *et al*. Retrieving effective parameters for metamaterials at oblique incidence. *Phys. Rev. B* **77**, 195328 (2008).

3. Markos, P. & Soukoulis, C. M., Transmission properties and effective electromagnetic parameters of double negative metamaterials, *Opt. Express* 11, 649-661 (2003).

4. Burgos, S. P., Waele, R., Polman, A. & Atwater, H. A. A single-layer wide-angle negative-index metamaterial at visible frequencies. *Nat. Mater.* **9**, 407-412 (2010).

5. Landau, L. D., Pitaevskiĭ, L. P. & Lifshitz, E. M., Electrodynamics of Continuous Media, 2nd Edition, 272-274, *Pergamon Press*, New York (1984).

6. Koschny, T., Markos, P., Smith, D. R. & Soukoulis, C. M., Resonant and antiresonant frequency dependence of the effective parameters of metamaterials. *Phys. Rev. E* **68**, 065602(R) (2003).

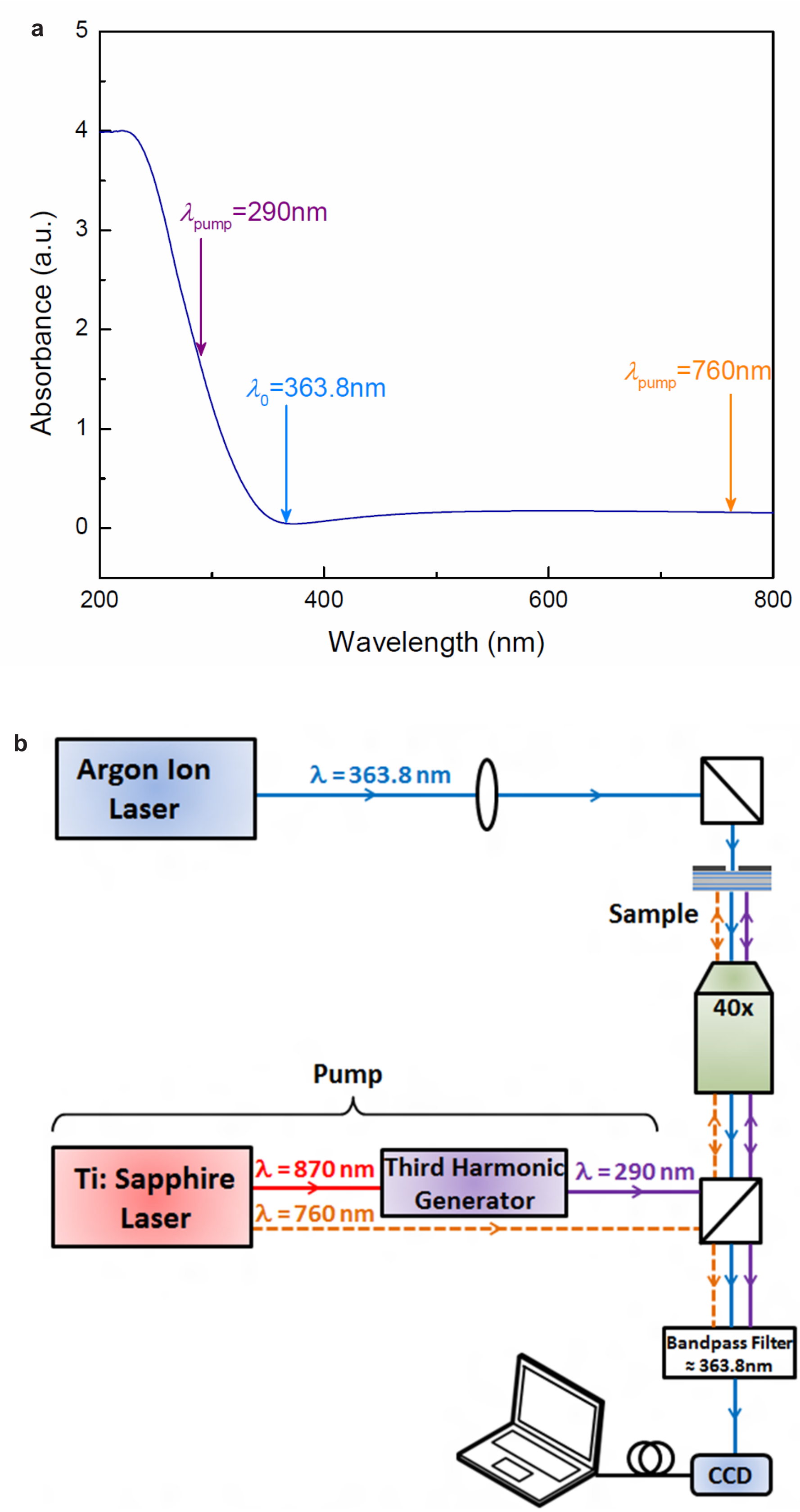

Figure 3 | Active Flat Lensing Experiment. a, Measured absorbance of 50nm-thick TiO_2 film, using UV-Visible spectrometer. **b,** Schematic of experimental setup used to demonstrate active flat lensing.